Lithographic antennas at visible frequencies

Christophe Fumeaux, Javier Alda, and Glenn D. Boreman

School of Optics and Center for Research and Education in Optics and Lasers, University of Central Florida, P.O. Box 162700, Orlando, Florida 32816-2700

Received May 17, 1999

The response of antenna-coupled thin-film Ni–NiO–Ni diodes to 633-nm helium–neon laser radiation is investigated. Although these detectors and their integrated dipole antennas are optimized for the detection of mid-infrared radiation, a polarization dependence of the measured response to visible radiation is observed. The strongest signals are measured for the polarization parallel to the dipole antenna axis, which demonstrates antenna operation of the device in the visible in addition to the expected thermal and photoelectric effects. The connection structure of the diode also resonates and contributes to the polarization-dependent signal. The receiving area of the dipole antenna is approximately 2 μm^2. © 1999 Optical Society of America

OCIS codes: 040.0040, 040.1880, 040.3060, 230.3990, 230.5440.

The efficiency of lithographic antennas has been demonstrated to mid-infrared frequencies.[1–3] The behavior of these antennas differs from that of their counterparts at lower frequencies primarily because of the reactive component of the surface impedance of the metals,[4] which also limits the high-frequency operation of antenna-coupled detectors designed for the infrared. As a confirmation, the metal whisker of a point-contact metal–oxide–metal (MOM) diode is an efficient long-wire antenna down to at least a wavelength of 10 μm but does not seem to act as an antenna for visible radiation.[5,6] Detection with MOM diodes in the visible has been attributed to photoconductive and thermal effects.[7] Correspondingly, to the best of our knowledge, no planar structure was previously shown to resonate as an antenna at visible wavelengths. In this study we have measured a polarized response of a thin-film antenna-coupled Ni–NiO–Ni diode at a wavelength of 632.8 nm. The highest responsivity occurs for radiation polarized parallel to the axis of the dipole antenna integrated with the MOM diode. Antenna structures for visible wavelengths would find applications in metrology for heterodyne detection in the visible,[8] real-time polarization-sensitive imaging, and near-field imaging.[9] Because the device that we measured was designed for an antenna resonance near 10 μm, we believe that the antenna response observed in the visible could be improved by optimization of the structure size for shorter wavelengths.

The sensors used in this study were thin-film MOM diodes with integrated dipole antennas[10] (Fig. 1, inset). A 3.5-nm NiO layer was sputtered between the separate depositions of the two Ni arms. The patterns were defined with electron-beam lithography, resulting in minimum feature sizes of approximately 0.2 μm. The substrate was Si, coated with a 1.5-μm layer of thermally grown SiO_2. The electrical connections to the diode are also depicted in the inset of Fig. 1. The dipole antenna had a total length of 6.7 μm.

The experimental setup used a linearly polarized He–Ne laser chopped at a frequency of 400 Hz. The linear polarization was rotated by means of a half-wave plate. After spatial filtering, expansion, and collimation, the beam was closely Gaussian, with a $1/e^2$ radius of 4 mm. This expanded beam was focused on the diode by a doublet lens with a focal length of 40 mm and an aperture of 22-mm diameter. The diode was mounted upon a three-axis positioning stage. The z direction (along the beam axis) was moved manually, and the x and y axes were motorized by a Melles Griot Nanomover system with a bidirectional repeatability of 100 nm. The diode was initially place approximately at the focus of the beam. We maximized the response by moving the device along the three directions, placing the device at the point of highest irradiance. At visible frequencies the devices were illuminated from the air side because the Si substrate is opaque. The use of a transparent substrate such as quartz would permit illumination from the substrate side and would enhance the antenna's performance in the visible.

We measured the polarization dependence of the response of the Ni–NiO–Ni detector by rotating the half-wave plate of 180° in 4° steps (Fig. 1). The signal was

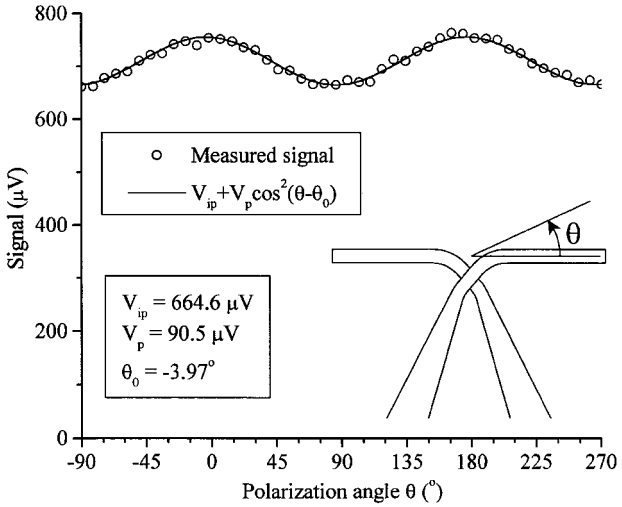

Fig. 1. Polarization dependence of the signal measured with an antenna-coupled Ni–NiO–Ni diode illuminated with 633-nm wavelength radiation.

0146-9592/99/221629-03$15.00/0

fitted to the sum of a constant V_{ip} and a cosine squared function with an amplitude V_p. The maximum signal was measured at an angle θ_0 close to zero, corresponding to polarization parallel to the antenna axis. The deviation of the value of $\theta_0 = -3.97°$ from zero can be explained by the mounting tolerances of the detectors on their chip carriers and by the uncertainties of the angular orientation of the polarizing elements. The polarization-dependent contribution to the signal is evidence of an antenna effect in the visible.

In addition to the dipole-antenna response, a response from the electrical connections to the diode was observed in all measurements. To investigate the antenna mechanism of this metallic V structure, we performed one-dimensional scans across these connections. The focused beam was scanned perpendicular to the line of symmetry of the connections, at a distance of 5 μm from the Ni–NiO–Ni diode (Fig. 2, inset). Comparing the data in Figs. 1 and 2, we can see that the responses from the two connections were less than 20% of the maximum detector response. The response of each connection can also be represented as the sum of a constant and a cosine squared oscillating with the polarization angle (Fig. 2). The two connections exhibit a maximum response for angles of $\theta_A = -12.7°$ and $\theta_B = 19.8°$, respectively. These angles correspond to the local cross-arm direction of the connections. The cross-arm dimension of the connections at this distance from the diode is of the order of 2λ, so the transverse modes of the arm influence the observed polarization dependence. This response of the electrical connection structure is more noticeable in our visible-wavelength experiments than in measurements reported at infrared frequencies.[1,2]

A precise characterization of the beam incident upon the detector is necessary to deconvolve the receiving area of our antenna-coupled detectors.[11] The beam profile at the point of highest irradiance was analyzed by knife-edge scans in the x and y directions. The incident beam was modeled based on the characteristics of the optical train, e.g., aperture of the last lens, radius of the beam before the last lens, and spherical aberration. Careful alignment permitted elimination of angular asymmetries in the beam. Thus the focused irradiance was modeled as a radial distribution, generated as a convolution of a Gaussian beam with an aberrated Airy disk containing only spherical aberration.[12] The beam parameters were obtained by use of a least-squares fitting procedure on the experimental knife-edge data. Ninety per cent of the beam energy in the plane of maximum irradiance was contained in a circular area with a radius of 3.2 μm.

The spatial response of the antenna-coupled detectors to visible radiation was obtained with a two-dimensional scanning and deconvolution process, similar to that described in Ref. 11 for infrared radiation at 10.6 μm. The Richardson–Lucy deconvolution algorithm permits retrieval of the spatial response of the detector from the measured data and from the modeled incident beam. The detectors were scanned across the beam in a 16 μm $\times$ 16 μm window, with 0.2-μm steps in both directions. The measurement was performed for the polarization parallel to the dipole axis and for the orthogonal polarization. We averaged three sets of data for each polarization direction, taking into account the symmetry of the antenna structure. The averaged response was deconvolved from the incident beam by 300 iterations. The results can be seen in Figs. 3(a) and 3(b). We have plotted the 10% and the 50% response levels to show that most of the receiving area is located close to the diode. The spatial response for the polarization parallel to the antenna [Fig. 3(a)] contains contributions from the dipole and from thermal effects. The location and shape of the contours for the cross-polarized spatial response [Fig. 3(b)], slightly displaced away from the dipole, indicate a nonnegligible antenna contribution of the V-shaped connection structure, besides the thermal response. Taking the signal difference between the two polarizations [Fig. 3(c)] cancels the contribution of the thermal and polarization-independent mechanisms. However, this operation also subtracts the polarization-dependent responses over the regions of their overlap. Therefore Fig. 3(c) cannot be considered as purely a dipole-antenna response. The individual spatial response of the dipole antenna [portion about the center of the dipole in Fig. 3(c)], disregarding the connections, is approximately an elliptical region with an axis ratio of roughly 3:2. A conservative estimate of the area where the dipole antenna collects most of the energy (90%) is approximately 2 μm^2. In the

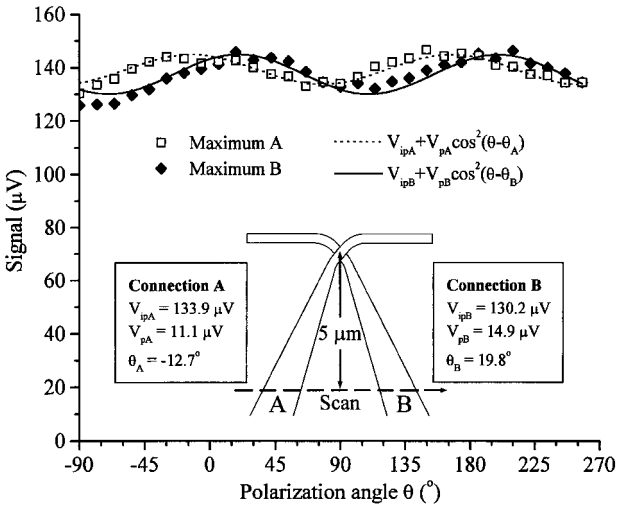

Fig. 2. Polarization dependence of the response of the connections to the diode.

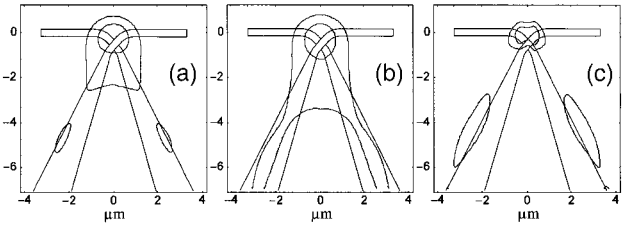

Fig. 3. Receiving area of the Ni–NiO–Ni diode for 633-nm radiation with polarization (a) parallel and (b) perpendicular to the antenna. (c) Difference between the parallel and the perpendicular polarizations. The contours correspond to 10% and 50% of the maximum value.

infrared case, at 10.6 μm, the collecting area extended approximately one dielectric wavelength past the dipole antenna in all directions.[11] On the contrary, in the visible the collecting area does not cover the entire dipole and is located in a small region about the center of the dipole. This confirms that the antenna currents are strongly attenuated at visible frequencies, hindering the development of strong resonances on the dipole antenna. Current waves will not propagate past one or two wavelengths because of this high attenuation. Therefore antenna structures intended for use at visible wavelengths must be fabricated with dimensions comparable with one wavelength. The large dimensions of the structure investigated, compared with the wavelength, and the deviation of the design from an ideal dipole antenna explain the observation that several locations on the devices show sensitivity to different polarizations.

Previous measurements[5,6] performed with visible radiation with point-contact MOM diodes did not point to any evidence of an antenna-coupling contribution. Detection and mixing in the visible were attributed to thermal and photoelectric effects. The large size of the metal whisker (typical diameter of 25 μm) relative to visible wavelengths gives a plausible explanation for the absence of the effect in those experiments. Similarly, experiments performed with planar MOM diodes fabricated with optical lithography did not demonstrate any antenna effect.[13] The lateral dimension of the antenna, of the order of 1 μm, and the structural roughness of these evaporated films compared with the wavelength explain the lack of an observable polarization-dependent signal. In our present experiments the thermal and photoelectric mechanisms are certainly present and contribute to the part of the signal that is independent of polarization. However, the small dimensions of our structures, with widths of approximately 200 nm, and the superior quality of the sputtered metal films compared with evaporated films permitted us to observe an antenna effect in the visible.

A polarization dependence of the signal measured with our detectors has demonstrated an antenna effect at visible frequencies. The results were obtained with planar antenna-coupled Ni–NiO–Ni diodes optimized for infrared radiation. The dipole antenna used in this study had a length of the order of 10 wavelengths of the incident radiation and a cross-arm width of the order of one third of that wavelength. The structure, which also contains large connections to the diode, is consequently overdimensioned. We have seen that the polarization dependence associated with the dipole antenna contribution is modified by other antenna contributions from the rest of the structure. A mapping of the antenna receiving area obtained from a two-dimensional scanning and a deconvolution from the incident beam confirms that antenna current waves at visible frequencies are strongly attenuated and extend only over a distance of one to two wavelengths. Overcoming this strong attenuation will be a major challenge in the development of efficient visible antennas. We believe that by appropriate scaling of the antennas, suitable choice of the substrate, and optimization of the geometry and dimensions of the contact structures a much stronger polarization dependence should be observable in the visible.

We are grateful to F. K. Kneubühl of the Swiss Federal Institute of Technology (ETH), Zürich. We acknowledge the support of the Ballistic Missile Defense Organization. J. Alda is supported by a scholarship (PR1997-0252) from the Ministerio de Educación y Cultura of Spain and by a grant from the School of Optics of the University of Central Florida. His permanent address is School of Optics, University Complutense of Madrid, Avda. Arcos de Jalón s/n, 28037 Madrid, Spain. The authors' e-mail addresses, in order, are cfumeaux@mail.creol.ucf.edu, j.alda@fis.ucm.es, and boreman@creol.ucf.edu.

References

1. I. Wilke, W. Herrmann, and F. K. Kneubühl, Appl. Phys. B **58,** 87 (1994).
2. C. Fumeaux, W. Herrmann, F. K. Kneubühl, and H. Rothuizen, Infrared Phys. Technol. **39,** 123 (1998).
3. E. N. Grossman, J. E. Sauvageau, and D. G. McDonald, Appl. Phys. Lett. **59,** 3225 (1991).
4. D. B. Rutledge, S. E. Schwarz, and A. T. Adams, Appl. Phys. **18,** 713 (1978).
5. S. Wang, Appl. Phys. Lett. **28,** 303 (1976).
6. O. Acef, L. Hilico, M. Bahoura, F. Nez, and P. De Natale, Opt. Commun. **109,** 428 (1994).
7. B.-I. Twu and S. E. Schwarz, Appl. Phys. Lett. **25,** 595 (1974).
8. H. Schnatz, B. Lipphardt, J. Helmcke, F. Riehle, and G. Zinner, Phys. Rev. Lett. **76,** 18 (1996).
9. R. D. Grober, R. J. Schoelkopf, and D. E. Prober, Appl. Phys. Lett. **70,** 1354 (1997).
10. I. Wilke, Y. Oppliger, W. Herrmann, and F. K. Kneubühl, Appl. Phys. A **58,** 329 (1994).
11. J. Alda, C. Fumeaux, I. Codreanu, J. A. Schaefer, and G. D. Boreman, Appl. Opt. **38,** 3993 (1999).
12. M. Born and E. Wolf, *Principles of Optics*, 6th ed. (Pergamon, London, 1980), Chap. 9.
13. M. Heiblum, S. Wang, J. R. Whinnery, and T. K. Gustafson, IEEE J. Quantum Electron. **QE-14,** 159 (1978).